Research Article | Vol. 26, No. 9 | 30 Apr 2018 | OPTICS EXPRESS 11928
Optics EXPRESS

Ultrafast multi-layer subtractive patterning

DANIEL J. HEATH,[1,*] TAIMOOR H. RANA,[2] RUPERT A. BAPTY,[2] JAMES. A GRANT-JACOB,[1] YUNHUI XIE,[1] ROBERT W. EASON,[1] AND BEN MILLS[1]

[1]*Optoelectronics Research Centre, University of Southampton, SO17 1BJ, UK*
[2]*School of Physics and Astronomy, University of Southampton, SO17 1BJ, UK*
**djh2v07@soton.ac.uk*

Abstract: Subtractive femtosecond laser machining using multiple pulses with different spatial intensity profiles centred on the same position on a sample has been used to fabricate surface relief structuring. A digital micromirror device was used as an intensity spatial light modulator, with a fixed position relative to the sample, to ensure optimal alignment between successive masks. Up to 50 distinct layers, 335 nm lateral spatial resolution and 2.6 µm maximum depth structures were produced. The lateral dimensions of the structures are approximately 40 µm. Surface relief structuring is shown to match intended depth profiles in a nickel substrate, and highly repeatable stitching of identical features in close proximity is also demonstrated.

OCIS codes: (140.3300) Laser beam shaping; (230.6120) Spatial light modulators; (220.4000) Microstructure fabrication.

References and links

1. E. G. Gamaly, A. V. Rode, B. Luther-Davies, and V. T. Tikhonchuk, "Ablation of solids by femtosecond lasers: Ablation mechanism and ablation thresholds for metals and dielectrics," Phys. Plasmas **9**(3), 949–957 (2002).
2. B. N. Chichkov, C. Momma, S. Nolte, F. von Alvensleben, and A. Tünnermann, "Femtosecond, picosecond and nanosecond laser ablation of solids," Appl. Phys., A Mater. Sci. Process. **63**(2), 109–115 (1996).
3. B. Mills, M. Feinaeugle, C. L. Sones, N. Rizvi, and R. W. Eason, "Sub-micron-scale femtosecond laser ablation using a digital micromirror device," J. Micromech. Microeng. **23**(3), 35005 (2013).
4. D. J. Heath, M. Feinaeugle, J. A. Grant-Jacob, B. Mills, and R. W. Eason, "Dynamic spatial pulse shaping via a digital micromirror device for patterned laser-induced forward transfer of solid polymer films," Opt. Mater. Express **5**(5), 1129 (2015).
5. D. J. Heath, B. Mills, M. Feinaeugle, and R. W. Eason, "Rapid bespoke laser ablation of variable period grating structures using a digital micromirror device for multi-colored surface images," Appl. Opt. **54**(16), 4984–4988 (2015).
6. M. Feinaeugle, D. J. Heath, B. Mills, J. A. Grant-Jacob, G. Z. Mashanovich, and R. W. Eason, "Laser-induced backward transfer of nanoimprinted polymer elements," Appl. Phys., A Mater. Sci. Process. **122**(4), 398 (2016).
7. C. Sun, N. Fang, D. M. Wu, and X. Zhang, "Projection micro-stereolithography using digital micro-mirror dynamic mask," Sens. Actuators A Phys. **121**(1), 113–120 (2005).
8. Z. Kuang, D. Liu, W. Perrie, S. Edwardson, M. Sharp, E. Fearon, G. Dearden, and K. Watkins, "Fast parallel diffractive multi-beam femtosecond laser surface micro-structuring," Appl. Surf. Sci. **255**(13-14), 6582–6588 (2009).
9. R. C. Y. Auyeung, H. Kim, S. Mathews, and A. Piqué, "Spatially modulated laser pulses for printing electronics," Appl. Opt. **54**(31), F70–F77 (2015).
10. B. Mills, D. J. Heath, M. Feinaeugle, J. Grant-Jacob, and R. W. Eason, "Laser ablation via programmable image projection for submicron dimension machining in diamond," J. Laser Appl. **26**(4), 41501 (2014).
11. D. J. Heath, J. A. Grant-Jacob, M. Feinaeugle, B. Mills, and R. W. Eason, "Sub-diffraction limit laser ablation via multiple exposures using a digital micromirror device," Appl. Opt. **56**(22), 6398–6404 (2017).
12. Texas Instruments, "DLP7000UV DLP® 0.7 UV XGA 2x LVDS Type A DMD," http://www.ti.com/lit/ds/symlink/dlp7000.pdf.
13. X. Ma, Y. Kato, F. Kempen, Y. Hirai, T. Tsuchiya, F. Keulen, and O. Tabata, "Multiple patterning with process optimization method for maskless DMD-based grayscale lithography," Procedia Eng. **120**, 1091–1094 (2015).
14. M. Zhang, Q. Deng, L. Shi, A. Cao, H. Pang, and S. Hu, "A Gray Matching Method for Cylindrical Lens Array Fabrication Based on DMD Lithography," Manip. Manuf. Meas. Nanoscale **127**, 145–147 (2016).
15. W. Iwasaki, T. Takeshita, Y. Peng, H. Ogino, H. Shibata, Y. Kudo, R. Maeda, and R. Sawada, "Maskless lithographic fine patterning on deeply etched or slanted surfaces, and grayscale lithography, using newly developed digital mirror device lithography equipment," Jpn. J. Appl. Phys. **51**(6S), 06FB05 (2012).

#326130 https://doi.org/10.1364/OE.26.011928
Journal © 2018 Received 15 Mar 2018; revised 28 Mar 2018; accepted 29 Mar 2018; published 24 Apr 2018

Optics EXPRESS

16. Y. Lu, G. Mapili, G. Suhali, S. Chen, and K. Roy, "A digital micro-mirror device-based system for the microfabrication of complex, spatially patterned tissue engineering scaffolds," J. Biomed. Mater. Res. A **77**(2), 396–405 (2006).
17. K. R. Kim, J. Yi, S. H. Cho, N. H. Kang, M. W. Cho, B. S. Shin, and B. Choi, "SLM-based maskless lithography for TFT-LCD," Appl. Surf. Sci. **255**(18), 7835–7840 (2009).
18. K. Zhong, Y. Gao, F. Li, N. Luo, and W. Zhang, "Fabrication of continuous relief micro-optic elements using real-time maskless lithography technique based on DMD," Opt. Laser Technol. **56**, 367–371 (2014).
19. M. V. Kessels, C. Nassour, P. Grosso, and K. Heggarty, "Direct write of optical diffractive elements and planar waveguides with a digital micromirror device based UV photoplotter," Opt. Commun. **283**(15), 3089–3094 (2010).
20. D. J. Heath, J. A. Grant-Jacob, R. W. Eason, and B. Mills, "Single-pulse ablation of multi-depth structures via spatially filtered binary intensity masks," Appl. Opt. **57**(8), 1904–1909 (2018).
21. K. Venkatakrishnan, B. Tan, and B. K. A. Ngoi, "Femtosecond pulsed laser ablation of thin gold film," SPIE **2403**, 199–202 (1995).
22. J. A. Grant-Jacob, B. Mills, M. Feinaeugle, C. L. Sones, G. Oosterhuis, M. B. Hoppenbrouwers, and R. W. Eason, "Micron-scale copper wires printed using femtosecond laser-induced forward transfer with automated donor replenishment," Opt. Mater. Express **3**(6), 747–754 (2013).
23. A. Mathis, F. Courvoisier, L. Froehly, L. Furfaro, M. Jacquot, P. A. Lacourt, and J. M. Dudley, "Micromachining along a curve: Femtosecond laser micromachining of curved profiles in diamond and silicon using accelerating beams," Appl. Phys. Lett. **101**(7), 99–102 (2012).
24. A. F. Courtier, J. A. Grant-Jacob, R. Ismaeel, D. J. Heath, G. Brambilla, W. J. Stewart, R. W. Eason, and B. Mills, "Laser-Based Fabrication of Nanofoam inside a Hollow Capillary," Mater. Sci. Appl. **8**(12), 829–837 (2017).
25. Texas Instruments, "DLP 0.3 WVGA Series 220 DMD," (2014).
26. J. Sudagar, J. Lian, and W. Sha, "Electroless nickel, alloy, composite and nano coatings - A critical review," J. Alloys Compd. **571**, 183–204 (2013).
27. L. Yang, Y. Ding, B. Cheng, A. Mohammed, and Y. Wang, "Numerical simulation and experimental research on reduction of taper and HAZ during laser drilling using moving focal point," Int. J. Adv. Manuf. Technol. **91**(1-4), 1171–1180 (2017).
28. M. S. Miller, M. A. Ferrato, A. Niec, M. C. Biesinger, and T. B. Carmichael, "Ultrasmooth gold surfaces prepared by chemical mechanical polishing for applications in nanoscience," Langmuir **30**(47), 14171–14178 (2014).
29. J. J. J. Kaakkunen, M. Silvennoinen, K. Paivasaari, and P. Vahimaa, "Water-assisted femtosecond laser pulse ablation of high aspect ratio holes," Phys. Procedia **12**, 88–93 (2011).
30. J. Bonse, J. Krüger, S. Höhm, and A. Rosenfeld, "Femtosecond laser-induced periodic surface structures," J. Laser Appl. **24**(4), 42006 (2012).
31. E. G. Gamaly, A. V. Rode, B. Luther-Davies, and V. T. Tikhonchuk, "Ablation of solids by femtosecond lasers: Ablation mechanism and ablation thresholds for metals and dielectrics," Phys. Plasmas **9**(3), 949–957 (2002).
32. J. A. Grant-Jacob, B. Mills, and R. W. Eason, "Parametric study of the rapid fabrication of glass nanofoam via femtosecond laser irradiation," J. Phys. D Appl. Phys. **47**(5), 55105 (2014).
33. H. Bostanci, V. Singh, J. P. Kizito, D. P. Rini, S. Seal, and L. C. Chow, "Micro Scale Surface Modifications for Heat Transfer Enhancement," ACS Appl. Mater. Interfaces **5**(19), 9572–9578 (2013).
34. L. Romoli, G. Tantussi, and G. Dini, "Experimental approach to the laser machining of PMMA substrates for the fabrication of microfluidic devices," Opt. Lasers Eng. **49**(3), 419–427 (2011).
35. T. Tamulevičius, R. Šeperys, M. Andrulevičius, and S. Tamulevičius, "Laser beam shape effect in optical control of the μ-fluidic channel depth employing scatterometry," Opt. Lasers Eng. **48**(6), 664–670 (2010).
36. J. C. McDonald, D. C. Duffy, J. R. Anderson, D. T. Chiu, H. Wu, O. J. Schueller, and G. M. Whitesides, "Review General Fabrication of microfluidic systems in poly(dimethylsiloxane)," Electrophoresis **21**(1), 27–40 (2000).
37. S. A. M. Shaegh, A. Pourmand, M. Nabavinia, H. Avci, A. Tamayol, P. Mostafalu, H. B. Ghavifekr, E. N. Aghdam, M. R. Dokmeci, A. Khademhosseini, and Y. S. Zhang, "Rapid prototyping of whole-thermoplastic microfluidics with built-in microvalves using laser ablation and thermal fusion bonding," Sens. Actuators B Chem. **255**, 100–109 (2018).

1. Introduction

The reduced heat affected zone offered by femtosecond laser machining, in comparison to nanosecond and longer laser pulses, allows for high precision sub-micron scale manufacturing [1,2]. By using a dynamic intensity mask, such as a digital micromirror device (DMD), femtosecond laser machining has previously been shown to produce complex two-dimensional patterns via individual laser pulses [3–10]. The ability to update intensity masks on a millisecond timescale lends considerable flexibility over other laser surface-patterning techniques, such as raster-scanning a focused spot, and provides a great speed of production advantage over the use of multiple static masks [11]. Extremely high-speed beam shaping is

Optics EXPRESS

possible with DMDs, which have a refresh rate of over 30 kHz in some models [12]. As the DMD surface consists of an array of 'off' or 'on' mirrors, typically, only binary intensity control is offered. Without further adaptation, this approach will therefore lead to only one depth of ablation when exposures are made using DMDs as intensity masks. Further techniques must be employed to obtain more complex surface relief structuring.

Others have demonstrated additive complex surface relief structuring, though these relied on the exposure of photoresists over long timescales, where grayscale intensities were achieved by averaging the 'dithering' of DMD mirrors over a several-second timescale [13–19]. This approach would not be appropriate in this case, as a femtosecond pulse is short in comparison to a single refresh cycle of the DMD mirrors. We have previously demonstrated a digital holographic technique for achieving multiple depths of ablation in a single femtosecond exposure, with lateral resolutions on the scale of 2 µm, and depths achieved were typically on the 100 nm scale [20], but required precise alignment through, and modelling of, apertures in the system. In this work, by using repeated exposures of less complex masks, complex structures can be fabricated with depths of ~3 µm. By employing multiple pulses, an enhanced lateral resolution is also achievable over that which is possible in a single exposure, with a minimum of 335 nm in electroless nickel, close to the limit found previously in this material [11]. While electroless nickel was chosen here due to its amorphous structure, to eliminate grain boundary effects, femtosecond exposures of DMD masks have been used to ablate a wide range of materials previously [1,4,10,21–24], including other metals, semi-conductors, glasses, and typically difficult to machine materials, such as diamond. The method presented here is expected to be applicable in the same range of materials, though the specific resolution and depth limits will vary.

2. Experimental Setup

A 1 mJ, 150 fs pulse length, 1 kHz repetition rate, 800 nm wavelength Ti:sapphire amplifier, provided laser pulses that were spatially homogenized (Pi-Shaper 6_6) and then spatially shaped by a DMD (Texas Instruments DLP3000) [25]. A 50x objective lens demagnified the shaped pulses onto the surface of an electroless nickel sample (5 µm electroless nickel layer deposited on copper [26], obtained commercially from LBP Optics Ltd.) where the pattern on the DMD was reproduced via ablation (up to small diffractive differences caused by spatial filtering [20]). Subsequent exposures using different masks, targeted at the same sample position, then removed additional material in order to produce a complex relief structure. Figure 1 demonstrates the concept and shows the shape of four sequential laser pulses (shown as purple, blue, green, yellow squares of different sizes) that would result in the fabrication of an inverted pyramid with four discrete layers. Bespoke masks can be used to build up more complex structures.

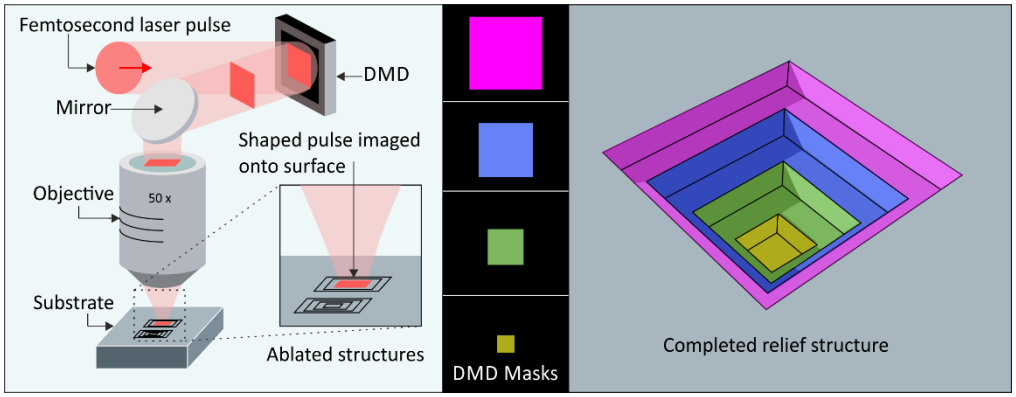

Fig. 1. (left) Schematic of the technique. (centre) Four sequentially smaller square DMD masks used for shaping the laser pulses. (right) Resultant inverted pyramid relief structure.

Optics EXPRESS

3. Experimental Results and Discussion

Experimental results of the patterning of an inverted pyramid structure with a fluence at the sample of ~1.8 J/cm^2 in electroless nickel are shown at various stages in Fig. 2. Both scanning electron microscope (SEM) images and interferometrically measured (Zygo Zescope, accurate to 0.1 nm depth measurements) profiles are shown. Square intensity masks, with a uniform reduction in width of 20 DMD mirrors, were exposed. Figures 2 (a)-2(c) shows the structure during the creation of a 20-level relief structure, with maximum depth 2.3 µm, with lateral resolution of ~950 nm. While the limit of final lateral resolution in this material (electroless nickel) was observed to benefit from the multiple exposure technique explored previously [11], with a minimum resolution of 335 nm, and ~400 nm shown in Fig. 3(a), the result in Fig. 2 demonstrates the applicability of this process for rapid manufacture of complex, high-fidelity structures in a case where the spatial resolutions created would not be a limiting factor.

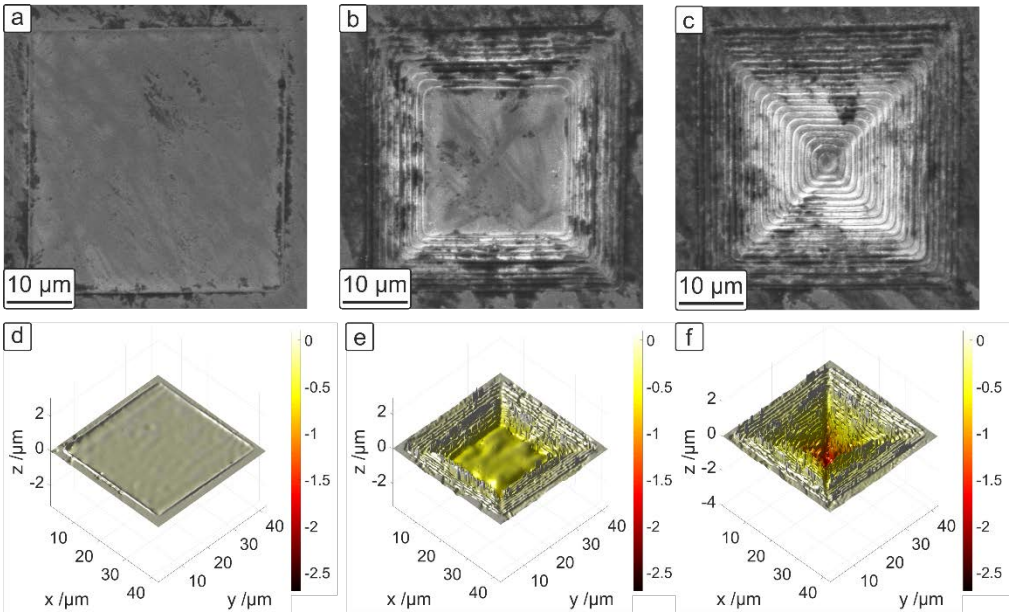

Fig. 2. Stages of production of a 20-layer inverted pyramid, with SEM images shown in (a-c) after a) 1, b) 10 and c) 20 layers. (d-f) show the corresponding interometrically measured depth profiles of the structures. The colour scale has been set equally across each image (d-f), to highlight the change in depth achieved with successive pulses.

Figure 3 shows results from the technique when applied to a variety of more complex depth profiles. Figure 3 (a) shows a pyramid structure at the base of a trench with sloped side-walls with 50 layers. The theoretical diffraction limit of the setup is 952nm (NA = 0.42), and the observed resolution of the step spacing here is ~400nm. The minimum resolution found with the technique was 335 nm, measured by averaging over several modulations in SEM images, and agrees with the previously observed multiple-exposure resolution reductions below the single-exposure limit observed in this material [11]. Figures 3(b) and 3(c) show an inverted dome and spire structure, respectively. The machined profiles (where machined depths are taken as the average of all positions exposed to the same number of pulses) are a close fit to the idealised versions (the profile expected if each DMD mask exposure were demagnified exactly at the sample, ablating a uniform depth), shown in Figs. 3(d)-3(f), and demonstrate the ability to generate structures with arbitrary depth profiles. The depth of the idealised version in each case has been normalised to the maximum depth observed in the machined sample. The slight disparity noticeable in (a) is likely due to interference effects

Optics EXPRESS

when projecting an image deep into a concave material surface [27]. The surface roughness of the structures (caused by debris redeposited after ablation) would likely benefit from chemical mechanical polishing [28] post-process, or a gas or water-assist removal of debris during machining [29]. Interferometric measurements are shown in Fig. 3(g)-3(i) to emphasise the 3D profile of the produced structures. The fluence at the sample was a) 1.8J/cm^2, and b-c) 0.9J/cm^2.

Though each of the shown structures were achieved via fluences between 0.9 J/cm^2 and 1.8 J/cm^2, this fluence range represented the limits of the technique on the optical setup. Fluences above 1.8 J/cm^2 approach the damage threshold at the DMD, while repeated exposures at fluences below 0.9 J/cm^2 resulted in laser-induced periodic surface structuring (LIPSS) [30], which reduced the fidelity of the step-like structuring seen in this work. The interference effects mentioned earlier when projecting deep into a concave surface [27] were the ultimate limiting factor on depth of machining, rather than layer number. However, when combined with the requirement of a minimum fluence to avoid LIPSS, an approximate limit of 50 exposures while maintaining acceptable fidelity of machining was found.

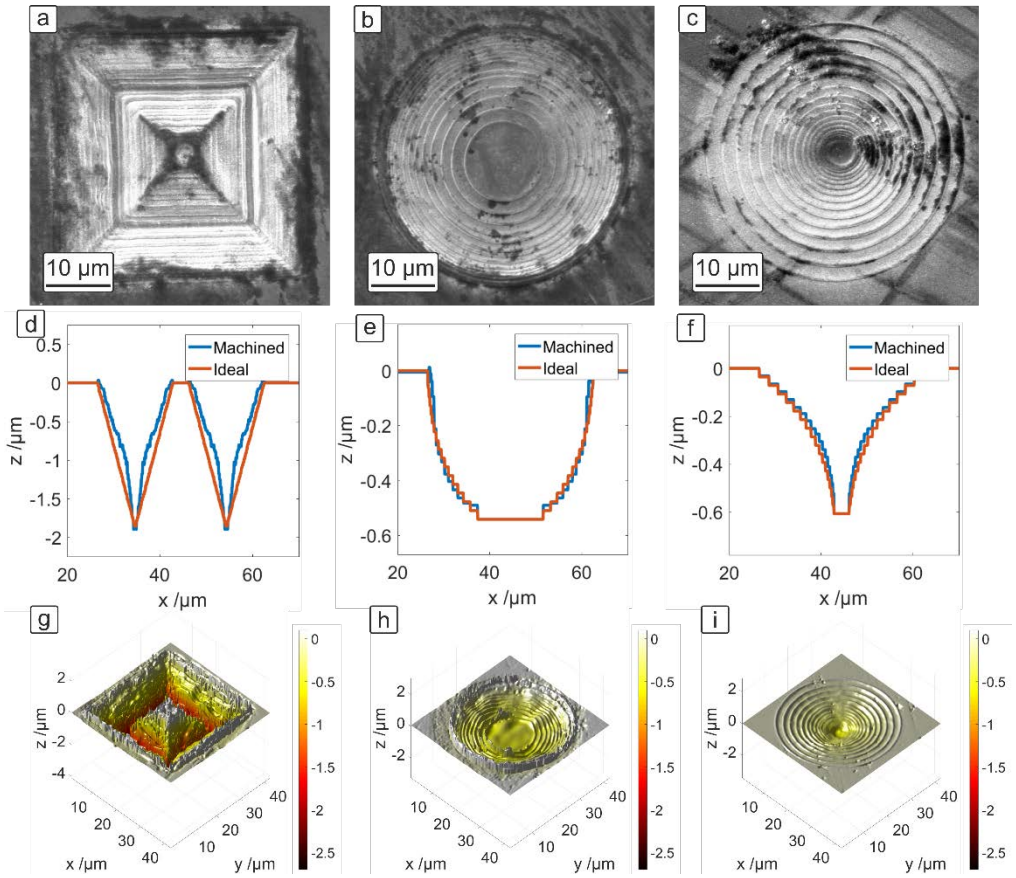

Fig. 3. SEM images for a) a 50-layer upright pyramid at the bottom of a sloped walled trench, b) a 17-layer inverted dome, c) a 17-layer inverted spire. Also showing the associated d-f) measured and ideal profiles and g-i) interferometric measurements for the produced structures.

Femtosecond pulses allow for higher fidelity machining than longer pulses. The subtractive removal of material via longer-pulsed laser ablation can often result in debris surrounding the machined region, which can be detrimental to the production of nearby, similar structures. Additionally, shocks and heat-affected zones in laser machining can be problematic for the integrity of closely-packed patterning. To demonstrate the circumvention

Optics EXPRESS

of these problems that are possible with femtosecond exposures (which have a limited heat-affected zone, and are typically less damaging to adjacent structures than nanosecond and longer pulses [31], though other forms of debris may be resultant [32]), an array of closely-packed, near-identical pyramid structures was produced. Each pyramid structure was completed before beginning the machining of adjacent structures. The resulting 10 × 10 grid of highly repeatable, ~2.6 µm deep structures are shown in Fig. 4, with interferometric 3D scans of the region, including a close up of a single structure. The fluence used for each exposure was 1.2 J/cm^2, and 40 exposures (40 separate masks with 1 exposure each) were used in total per pyramid.

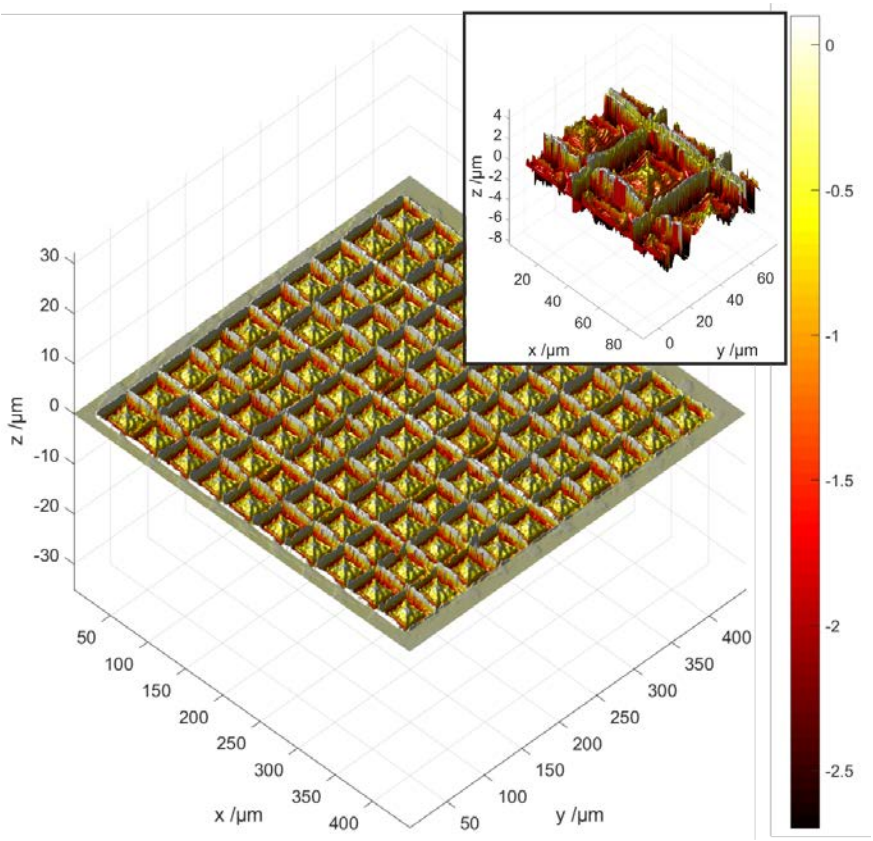

Fig. 4. The interferometric measurement of the machined array of 10 × 10 pyramid structures, with a close-up view of a single structure within the array shown as an inset to the figure.

4. Conclusions

We have demonstrated a method for highly repeatable subtractive laser-based machining of surface relief structures with high resolution features. Using a DMD as an intensity mask enabled the fabrication of up to 50 distinct layers, with minimum lateral resolution 335 nm and overall width of ~40 µm on a nickel substrate. A closely-packed array of such structures showed the technique's high repeatability. The fabrication of multi-level structures with features of this scale may have applications in areas such as microfluidics, security tagging and identification [10], and the manufacture of electronic components [33–37].

Acknowledgements

This work was supported under EPSRC grant numbers EP/N03368X/1 and EP/N509747/1. Supporting data for this submission can be found at https://doi.org/10.5258/SOTON/D0441.